arXiv:1609.07640v1 [cond-mat.str-el] 24 Sep 2016

Inelastic Kondo-Andreev tunnelings in a vibrating quantum dot

Zhan Cao,[1] Tie-Feng Fang,[1,*] Qing-Feng Sun,[2,3] and Hong-Gang Luo[1,4,†]

[1] *Center for Interdisciplinary Studies and Key Laboratory for Magnetism and Magnetic Materials of the Ministry of Education, Lanzhou University, Lanzhou 730000, China*
[2] *International Center for Quantum Materials, School of Physics, Peking University, Beijing 100871, China*
[3] *Collaborative Innovation Center of Quantum Matter, Beijing 100871, China*
[4] *Beijing Computational Science Research Center, Beijing 100084, China*

Phonon-assisted electronic tunnelings through a vibrating quantum dot embedded between normal and superconducting leads are studied in the Kondo regime. In such a hybrid device, with the bias applied to the normal lead, we find a series of Kondo sidebands separated by half a phonon energy in the differential conductance, which are distinct from the phonon-assisted sidebands previously observed in the conventional Andreev tunnelings and in systems with only normal leads. These Kondo sidebands originate from the Kondo-Andreev cooperative cotunneling mediated by phonons, which exhibit a novel Kondo transport behavior due to the interplay of the Kondo effect, the Andreev tunnelings, and the mechanical vibrations. Our result could be observed in a recent experiment setup [J. Gramich *et al.*, PRL **115**, 216801 (2015)], provided that their carbon nanotube device reaches the Kondo regime at low temperatures.

PACS numbers: 73.23.-b, 74.45.+c, 73.63.Kv, 71.38.-k

Introduction.— The hybrid quantum systems have a potential to exhibit new emergent phenomena through merging the strength of different media [1]. A quantum dot (QD) embedded between normal (N) and s-wave superconducting (S) leads (N-QD-S) is one of such devices, which has received considerable attentions from both the theoretical [2–11] and experimental [12–14] communities in the past two decades. In such a hybrid system, two important phenomena may arise: one is the Andreev tunneling (AT) [15] and the other is the screening of the localized spin in the QD by conduction electrons in the leads. While the former induces the Andreev bound states (ABSs) located in the supreconducting gap, the latter is the famous Kondo effect [16]. The competition between these two processes results in a profound influence on the ground state properties [5–11] as well as the transport behaviors of the devices [2–8, 10, 11].

For a molecular QD, it was found that vibrational degrees of freedom are easily excited when electronic tunneling takes place [17–19], which has a dramatic influence on the transport of the system due to the presence of inelastic tunneling processes mediated by emission or absorption of phonons [20–23]. In recent years, phonon-assisted inelastic AT in an N-QD-S system also leads to interesting physics on, for example, the electronic transport [24–26], the heat generation [27], the ground-state cooling [28], the steady-state shot noise [29], as well as the transient dynamics under a step bias [30]. More interestingly, the phonon-assisted AT can lead to resonant peaks every time the bias voltage changes by one phonon energy or the gate voltage changes by half a phonon energy [31, 32], which has been unambiguously observed in a recent experiment [33]. This is somewhat reminiscent of normal systems where phonon sidebands of Kondo cotunnelings [34–36] and single-electron tunnelings [37–39] are also separated by one phonon energy in the bias voltage. Since the N-QD-S setup fabricated in the experiment [33] is indeed an ideal platform to explore the Kondo physics, it is our aim in this paper to provide a theoretical study of the Kondo transport in such a device.

Our investigation reveals that the interplay of the Kondo correlations, the superconductivity, and the mechanical vibrations of the QD gives rise to distinct transport characteristics, as compared with those arising from the conventional phonon-assisted ATs [31–33]. The main physical scenario is illustrated in Fig. 1, where elastic and inelastic AT with and without the Kondo effect are schematically shown. We set the chemical potentials of the N (μ_N) and S (μ_S) leads as $\mu_N = V$, $\mu_S = 0$, and the superconducting gap Δ is taken as the largest energy scale in the problem. We consider the parameter regime where the QD-S tunnel coupling is much larger than the N-QD coupling and both are several times smaller than the onsite Coulomb repulsion, such that the Kondo effect and the onsite pairing coexist [14]. In this case, two Andreev bound states (ABSs) separated roughly by the Coulomb energy form at $\pm E_A$ and their widths are determined by the N-QD coupling [7]. At zero bias $V = 0$, a spin-$\uparrow$ localized electron and a spin-$\downarrow$ lead electron at μ_N can convert to a Cooper pair in S, while another spin-$\downarrow$ lead electron at μ_N transits into the QD simultaneously [Fig. 1(a)]. This spin-flip cotunneling process, to which we refer as the Kondo-Andreev tunneling, is elastic and accounts for the zero-bias conductance peak previously observed in this system [12, 14]. When the bias increases to $V = \varepsilon_{ph}/2$ (ε_{ph} the phonon energy), besides the elastic Kondo-Andreev tunneling process, additional inelastic Kondo-Andreev tunneling emitting one phonon can also take place [Fig. 1(b)]. Here, the emission of a phonon fulfills the energy conservation of the transition

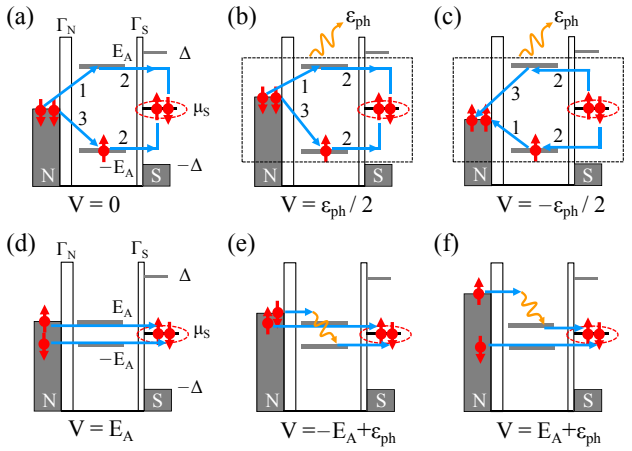

FIG. 1. (Color online) Schematics of elastic [(a), (d)] and inelastic [(b), (c), (e), (f)] electronic tunnelings in an N-QD-S system. (a)-(c) represent the Kondo-Andreev tunnelings through an interacting QD with the numbers 1, 2, 3 denoting the tunneling sequences. (d)-(f) show the conventional AT through a noninteracting QD. The wavy arrows represent the emission of phonons during the inelastic tunnelings.

that two N-lead electrons each with energy $\varepsilon_{ph}/2$ in the initial state are annihilated and a Cooper pair with zero energy is created in the final state, while the QD energy under the spin flipping remains the same. At negative bias $V = -\varepsilon_{ph}/2$, similar inelastic Kondo-Andreev tunneling can occur from the S lead to the N lead [Fig. 1(c)]. The opening of these additional tunneling channels would give rise to additional conductance peaks at $V = \pm\varepsilon_{ph}/2$. When multiple-phonon processes are involved, a series of sidebands separated by half a phonon energy are thus expected at $V = n\varepsilon_{ph}/2$ with $n = 0, \pm1, \pm2\cdots$.

For comparison, we also give a general scenario of the conventional phonon-assisted ATs for a noninteracting N-QD-S, where the QD without the onsite Coulomb interaction favors even electron occupation. In this system, there are two interleaved sets of phonon sidebands, each separated by ε_{ph}, in the differential conductance, since additional phonon-emitted inelastic AT can be triggered at $V = \pm E_A + n\varepsilon_{ph}$. For $n = 0$, the AT is elastic [see Fig. 1(d) for $V = E_A$]. For $n > 0$, an N-lead electron at μ_N can transfer to the S lead through the lower [Fig. 1(e), $V = -E_A + n\varepsilon_{ph}$] or upper [Fig. 1(f), $V = E_A + n\varepsilon_{ph}$] ABS by emitting n phonons, while another electron passes directly through the other ABS. Similar inelastic ATs take place from the S lead to the N lead for $n < 0$. When the two ABSs are indistinguishable (e.g., their widths being larger than their interval) or separated by multiples of ε_{ph}, the two sets of phonon sidebands merge into a single set of sidebands separated by one phonon energy. This is exactly the special case discussed in Ref. [31]. In the following, we perform a model calculation to demonstrate these transport scenarios.

Model and Formalism.—Our N-QD-S system is modeled by the Hamiltonian $H = H_{\rm leads} + H_{\rm ph} + H_{\rm QD} + H_{\rm tunnel}$. The first term represents the normal (β = N) and superconducting (β = S) leads, $H_{\rm leads} = \sum_{k,\sigma,\beta} \varepsilon_k c^\dagger_{k\sigma\beta} c_{k\sigma\beta} - \Delta \sum_k (c^\dagger_{k\uparrow S} c^\dagger_{-k\downarrow S} + c_{-k\downarrow S} c_{k\uparrow S})$. $H_{\rm ph} = \varepsilon_{ph} a^\dagger a$ models the local phonon mode. $H_{\rm QD} = \sum_\sigma \varepsilon_d d^\dagger_\sigma d_\sigma + U n_{d\uparrow} n_{d\downarrow} + \lambda(a + a^\dagger) \sum_\sigma n_{d\sigma}$ describes an interacting single-level QD, with Coulomb repulsion energy U, coupled with the local phonon by λ the Holstein-type electron-phonon interaction (EPI). The last term $H_{\rm tunnel} = \sum_{k,\sigma,\beta} (V_\beta c^\dagger_{k\sigma\beta} d_\sigma + {\rm H.c.})$ describes the electronic tunneling between the dot and the leads. From the tunneling matrix elements V_β, the dot level ε_d acquires an intrinsic broadening $\Gamma_\beta \equiv 2\pi\rho_0 |V_\beta|^2$ with ρ_0 the density of state of lead N and lead S in normal state. By the standard Keldysh nonequilibrium Green's function (GF) theory [40], the electronic current flowing from the N lead into the QD can be expressed as

$$I = \frac{2ie}{h} \int {\rm d}\omega\, \Gamma_{\rm N} [(1 - f_N) \mathbf{G}^<_{11}(\omega) + f_N \mathbf{G}^>_{11}(\omega)], \quad (1)$$

where $f_{\rm N}(\omega)$ is the Fermi distribution function of lead N. The boldfaced GF matrices are defined in the well-known 2×2 Nambu representation [41], from which the local density of states (LDOS) per spin can be calculated by $\rho(\omega) = -(1/\pi){\rm Im}\mathbf{G}^r_{11}(\omega)$.

In this work, we focus on the strong EPI regime. It is thus appropriate to make the non-perturbative Lang-Firsov transformation [42] $\tilde{H} = e^S H e^{-S}$ with $S = (\lambda/\varepsilon_{ph})(a^\dagger - a) \sum_\sigma n_{d\sigma}$ to eliminate the linear EPI. This gives us $\tilde{H} = H_{\rm leads} + H_{\rm ph} + \tilde{H}_{\rm QD} + \tilde{H}_{\rm tunnel}$, where $\tilde{H}_{\rm QD} = \sum_\sigma \tilde{\varepsilon}_d n_{d\sigma} + \tilde{U} n_{d\uparrow} n_{d\downarrow}$ and $\tilde{H}_{\rm tunnel} = \sum_{k,\sigma,\beta} (\tilde{V}_\beta c^\dagger_{k\sigma\beta} d_\sigma + {\rm H.c.})$, with $\tilde{\varepsilon}_d = \varepsilon_d - g\varepsilon_{ph}$, $\tilde{U} = U - 2g\varepsilon_{ph}$, $\tilde{V}_\beta = V_\beta X$, and $X = \exp[-(\lambda/\varepsilon_{ph})(a^\dagger - a)]$. Here a dimensionless measure of EPI $g \equiv \lambda^2/\varepsilon^2_{ph}$ is introduced. As in dealing with the localized polarons, we adopt the approximation replacing the operator X with its expectation value $\langle X \rangle = \exp[-g(N_{\rm ph} + 1/2)]$, where the average is taken over the independent phonon bath $H_{\rm ph}$, and $N_{\rm ph}$ is the Bose distribution. Hence, the renormalized $\tilde{\Gamma}_\beta = \langle X \rangle^2 \Gamma_\beta$. This approximation is valid when $V_\beta \ll \lambda$ and has been widely employed in both the N-QD-N [35, 37, 43] and N-QD-S systems [24–27, 29, 32]. Applying the above decoupling scheme and the Feynman disentangling technique [44], one obtains $\mathbf{G}^r_{11}(\omega) = \sum_{n=-\infty}^{\infty} L_n [\tilde{\mathbf{G}}^r_{11}(\omega - n\varepsilon_{ph}) + \frac{1}{2}\tilde{\mathbf{G}}^<_{11}(\omega - n\varepsilon_{ph}) - \frac{1}{2}\tilde{\mathbf{G}}^<_{11}(\omega + n\varepsilon_{ph})]$ and $\mathbf{G}^{<(>)}_{11}(\omega) = \sum_{n=-\infty}^{\infty} L_n \tilde{\mathbf{G}}^{<(>)}_{11}(\omega \pm n\varepsilon_{ph})$, where $L_n = \exp[-g(2N_{\rm ph} + 1)] \exp[n\beta\varepsilon_{ph}/2] I_n(x)$, with $x = 2g\sqrt{N_{\rm ph}(N_{\rm ph} + 1)}$ and $I_n(x)$ being the modified Bessel function of the first kind. Note that the new GFs $\tilde{\mathbf{G}}$ is defined according to the Hamiltonian $\tilde{H}$ in which the Bose degrees of freedom is totally decoupled.

We proceed to solve the retarded GF $\tilde{\mathbf{G}}^r(\omega)$ using the equation of motion method within the truncation scheme adopted by Sun *et al.* [3]. The solution of $\tilde{\mathbf{G}}^r(\omega)$, in the

large gap limit $\Delta \to \infty$, is obtained as

$$(\tilde{\mathbf{g}}_0^{-1} - \tilde{\mathbf{\Sigma}}_0^r - \tilde{U}\mathbf{PQ})\tilde{\mathbf{G}}^r = \mathbf{I} + \tilde{U}\mathbf{PN}, \qquad (2)$$

where $[\tilde{\mathbf{g}}_0^{-1}(\omega)]_{11} = \omega - \tilde{\varepsilon}_d$, $[\tilde{\mathbf{g}}_0^{-1}(\omega)]_{22} = \omega + \tilde{\varepsilon}_d$, $[\tilde{\mathbf{g}}_0^{-1}(\omega)]_{21} = [\tilde{\mathbf{g}}_0^{-1}(\omega)]_{12} = 0$, $\mathbf{P}_{11}(\omega) = (\omega + \tilde{\varepsilon}_d + \tilde{U} + 3i\tilde{\Gamma}_N/2)/\Omega(\omega)$, $\mathbf{P}_{22}(\omega) = -[\mathbf{P}_{11}(-\omega)]^*$, $\mathbf{P}_{12}(\omega) = \mathbf{P}_{21}(\omega) = -\tilde{\Gamma}_S/2\Omega(\omega)$, $\Omega(\omega) = (\omega - \tilde{\varepsilon}_d - \tilde{U} + 3i\tilde{\Gamma}_N/2)(\omega + \tilde{\varepsilon}_d + \tilde{U} + 3i\tilde{\Gamma}_N/2) - \tilde{\Gamma}_S^2/4$, $\mathbf{Q}_{11}(\omega) = -\sum_k \frac{|\tilde{V}_N|^2 f_N(\varepsilon_k)}{\omega - \varepsilon_k} - \sum_k \frac{|\tilde{V}_N|^2 f_N(\varepsilon_k)}{\omega + \varepsilon_k - 2\tilde{\varepsilon}_d - \tilde{U}}$, $\mathbf{Q}_{22}(\omega) = [\mathbf{Q}_{11}(-\omega)]^*$, $\mathbf{Q}_{12}(\omega) = -\mathbf{Q}_{21}(\omega) = -\tilde{\Gamma}_S/2$, $\mathbf{N}_{11} = \langle n_{d\downarrow}\rangle$, $\mathbf{N}_{22} = -\langle n_{d\uparrow}\rangle$, and $\mathbf{N}_{12} = \mathbf{N}_{21}^* = \langle d_\downarrow d_\uparrow\rangle$. The noninteracting retarded self-energy $\tilde{\mathbf{\Sigma}}_0^r$ can be exactly obtained [41]. Note that the elements of matrix $\mathbf{N}$ should be calculated by the equations $\langle n_{d\uparrow}\rangle = \langle n_{d\downarrow}\rangle = \int \frac{d\omega}{2\pi i}\tilde{\mathbf{G}}_{11}^<(\omega)$ and $\langle d_\downarrow d_\uparrow\rangle = \int \frac{d\omega}{2\pi i}\tilde{\mathbf{G}}_{12}^<(\omega)$, where the lesser and greater GFs are related to the retarded one through the kinetic equation $\tilde{\mathbf{G}}^{<(>)} = \tilde{\mathbf{G}}^r\tilde{\mathbf{\Sigma}}^{<(>)}\tilde{\mathbf{G}}^a$ with $\tilde{\mathbf{G}}^{\mathbf{a}} = (\tilde{\mathbf{G}}^{\mathbf{r}})^\dagger$. We further approximate the lesser and greater self-energies $\tilde{\mathbf{\Sigma}}^{<(>)}$ by their noninteracting counterparts $\tilde{\mathbf{\Sigma}}_0^{<(>)}$ [45, 46]. The formulae are thus closed, which can be self-consistently calculated to determine the GFs $\tilde{\mathbf{G}}^r$, $\tilde{\mathbf{G}}^<$, and $\tilde{\mathbf{G}}^>$, and subsequently the current I, differential conductance $G \equiv dI/dV$, and LDOS $\rho(\omega)$.

Results and discussions.—In the numerical results presented below, we take all the renormalized parameters to be freely tunable. $\tilde{\Gamma}_N$ is taken as the energy unit and the temperature is always set at zero. We consider first the phonon-assisted inelastic AT in the Kondo regime. To this end, we adopt the parameters $\tilde{\varepsilon}_d = -2.5$, $\tilde{\Gamma}_S = 4$, and $\tilde{U} = 10$ such that the Kondo effect and the on-dot paring coexist. In Fig. 2(a), it is shown that remarkable differential conductance peaks, in addition to the zero-bias Kondo peak, develop whenever the bias voltage varies by half a phonon energy. These Kondo sidebands are consistent with the scenarios previously discussed in Figs. 1(a)-(c), and are very different from those occurring in N-QD-N systems that are separated by one phonon energy [34–36]. Note also that the Kondo sidebands at positive bias are much weaker than those at negative bias, which can be ascribed to that the Kondo effect is suppressed (enhanced) at positive (negative) bias since the dot energy level gets away from (closer to) the Fermi level of lead N. Furthermore, as compared with the Kondo resonance at zero EPI [see the red dashed curve in Fig. 2(a)], the zero-bias peak at finite EPI is significantly reduced and narrowed.

The underlying physics about why the conductance peaks are separated by $\varepsilon_{ph}/2$ can be acquired by examining the LDOS, since the conductance from the Kondo-Andreev tunneling processes is roughly proportional to the convolution of electron and hole density of states [14, 47]. Fig. 2(b) presents the LDOS for several bias voltages decreasing in a step of $\varepsilon_{ph}/4$. In equilibrium, multiple Kondo satellites ($\omega = n\varepsilon_{ph}$) exhibit on each side

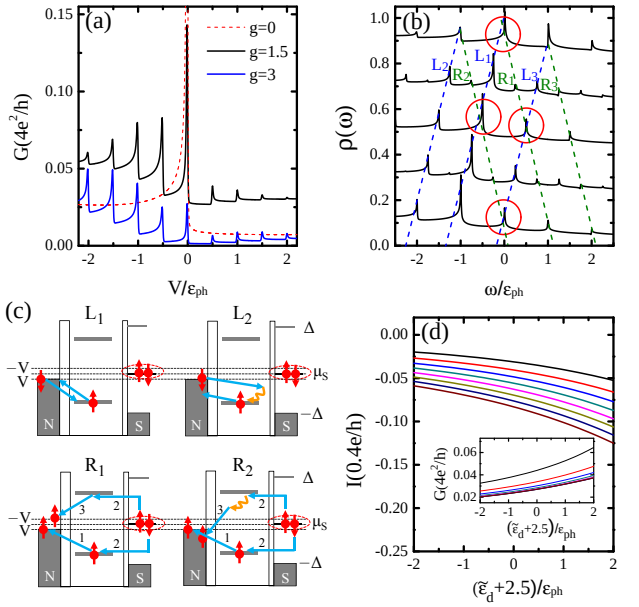

FIG. 2. (Color online) (a) Differential conductance in the Kondo regime with different EPI strength for $\tilde{\varepsilon}_d = -2.5$, $\tilde{\Gamma}_S = 4$, $\tilde{U} = 10$, and $\varepsilon_{ph} = 0.1$. The curve for $g = 1.5$ is offset by 0.025. (b) LDOS at different bias voltages $V = 0$ (top), $-\varepsilon_{ph}/4$, $-\varepsilon_{ph}/2$, $-3\varepsilon_{ph}/4$, and $-\varepsilon_{ph}$ (bottom). The curves are offset for clarity. The dashed lines guide the shift of the Kondo satellites, while the circles mark their mergence. (c) Illustrations of the Kondo cotunneling processes corresponding to the Kondo peaks in (b). (d) Currents vs $\tilde{\varepsilon}_d$ at different bias voltages (V decreases from $-\varepsilon_{ph}/4$ to $-2\varepsilon_{ph}$ by a step $\varepsilon_{ph}/4$, from top to bottom). Inset shows the corresponding differential conductance.

of the main Kondo resonance ($\omega = 0$) due to the EPI. In the following, we will focus on the nearest two satellites around the main resonance. In nonequilibrium, the main resonance and the two Kondo satellites all split into two subpeaks, resulting in totally six Kondo peaks in the LDOS as indicated by L_1 ($\omega = V$), L_2 ($\omega = V - \varepsilon_{ph}$), L_3 ($\omega = V + \varepsilon_{ph}$), R_1 ($\omega = -V$), R_2 ($\omega = -V - \varepsilon_{ph}$), and R_3 ($\omega = -V + \varepsilon_{ph}$) in Fig. 2(b). When the bias is tuned to $V = -\varepsilon_{ph}/2$, the two peaks L_1 and R_2, as well as L_3 and R_1, merge into a single pronounced resonance (marked by red circles), respectively. Clearly, the convolution of these two merged Kondo resonances is larger than the convolution of L_1 and R_1 at $V = -\varepsilon_{ph}/4$, thereby cooperatively giving rise to a conductance peak at $V = -\varepsilon_{ph}/2$. Similarly, at $V = -\varepsilon_{ph}$, the two Kondo satellites L_3 and R_2 get merged at $\omega = 0$ and thus results in a conductance peak. In short words, the Kondo sidebands always appear in the conductance at the bias voltage V under which the LDOS exhibits Kondo-peak cooperative enhancement within the bias window $\omega \in [-V, V]$.

The cotunneling processes associated with some Kondo peaks in the LDOS are illustrated in Fig. 2(c). It is shown that the cotunneling processes of the L_i ($i = 1, 2, 3$) and R_i Kondo peaks are of the second and fourth order, re-

spectively. This explains why the L_i Kondo resonances are stronger than the R_i resonances. Specifically, in the Kondo process of L_1, a localized spin-↑ electron tunnels out to lead N, followed closely by a spin-↓ electron at μ_N tunneling into the QD. At low temperatures, a coherent superposition of such second-order spin-flip cotunneling events yields a many-body spin singlet comprising of the localized and N-lead electrons, which manifests itself as the sharp Kondo resonance L_1 in the LDOS. When $\tilde{\Gamma}_S > \tilde{\Gamma}_N$ as in our case, the AT can also take part in the Kondo cotunneling process. For example, in the Kondo-Andreev process of R_1, the localized spin-↑ electron first tunnels out to μ_N and a Cooper pair in the S lead splits into two electrons with opposite spins. The split spin-↓ electron then tunnels into the QD while the other electron transfer through the QD to the empty state with energy $-V$ in lead N. The coherent superposition of such fourth-order spin-flip cotunneling events leads to the weak Kondo resonance R_1 in the LDOS [2, 3, 6]. Other Kondo peaks such as L_2, L_3, R_2, and R_3 are produced by similar Kondo and Kondo-Andreev cotunneling processes but with one phonon being emitted.

The current and conductance as a function of the dot level $\tilde{\varepsilon}_d$ are further investigated [Fig. 2(d)]. As we can see, both quantities change monotonously with $\tilde{\varepsilon}_d$. This is different from those in conventional AT regime where characteristic peaks show up whenever the the dot level $\tilde{\varepsilon}_d$ changes by $\varepsilon_{ph}/2$ [31, 33]. The featureless nature of our I vs $\tilde{\varepsilon}_d$ and G vs $\tilde{\varepsilon}_d$ curves can be readily understood. As long as $\tilde{\varepsilon}_d$ is always restricted in the Kondo regime, the resulting Kondo resonances are robust and no additional phonon-assisted channel could be opened or closed when $\tilde{\varepsilon}_d$ is varied.

For comparison, we now turn to investigate the conventional inelastic AT in a noninteracting ($\tilde{U} = 0$) N-QD-S with the QD level $\tilde{\varepsilon}_d = 0$ fixed at the Fermi energy. In this parameter regime, the two ABSs appear at $\pm E_A$ with $E_A = \tilde{\Gamma}_S/2$. In Figs. 3(a)-3(c), the conductance is displayed for three values of $\tilde{\Gamma}_S$. Different from the conductance behaviors in the Kondo regime, there are indeed two sets of phonon sidebands at $V_{\pm,n} \equiv \pm E_A + n\varepsilon_{ph}$, each separated by one phonon energy, in agreement with our previous discussions of Figs. 1(d)-1(f). Generally, the two sets of sidebands are interleaved [Figs. 3(a) and 3(b)]. For $E_A = \varepsilon_{ph}/2$ [Fig. 3(c)], the two sets of sidebands merge with each others. This corresponds to the I-V staircases addressed previously [31]. These conductance behaviors displayed can also be traced back to the LDOSs at different bias voltages, as shown in Figs. 3(d)-3(f). At zero bias, only hole-type (electron-type) sidebands of the upper (lower) ABS appear at $E_A + n\varepsilon_{ph}$ ($-E_A - n\varepsilon_{ph}$), with $n > 0$, which can be attributed to the fact that the upper (lower) ABS is fully empty (occupied) and the phonon absorption is unavailable at zero temperature [37]. For finite bias larger than E_A, the upper ABS becomes occupied, therefore phonon sidebands develop on both sides

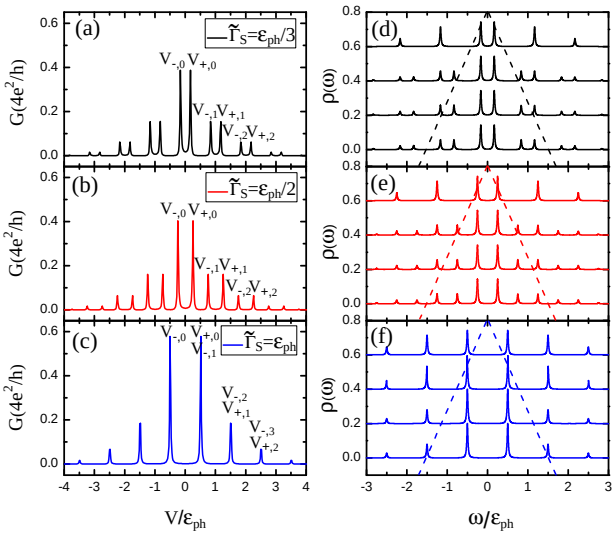

FIG. 3. (Color online) Left panel: the conductance of a noninteracting ($\tilde{U} = 0$) N-QD-S system with finite EPI $g = 0.8$ for different $\tilde{\Gamma}_S$ as indicated. Right panel: the corresponding LDOS at four different bias voltages $V = 0$, $\varepsilon_{ph}/2$, ε_{ph}, and $3\varepsilon_{ph}/2$ (from top to bottom in each figure). The curves are offset for clarity. The horizontal distance between the two dashed lines represents the bias window $\omega \in [-V, V]$. Other parameters are $\tilde{\varepsilon}_d = 0$ and $\varepsilon_{ph} = 30$.

of each ABS. Upon adjusting $\tilde{\Gamma}_S$ such that $E_A = n\varepsilon_{ph}/2$ the sidebands associated with the two ABSs merge together [see Fig. 3(f)].

Conclusions.—We have predicted in N-QD-S systems a series of differential conductance subpeaks developed at $V = n\varepsilon_{ph}/2$ and resulting from phonon-assisted inelastic Kondo-Andreev cotunnelings. These structure are truly remarkable when compared with the transport characteristics of i) the conventional inelastic AT in N-QD-S systems [31–33] and ii) the inelastic Kondo cotunneling in the N-QD-N systems [34–36]. Our prediction might be observed in the carbon nanotube device fabricated by J. Gramich *et al.* [33] as long as the Kondo regime is achieved at low temperatures. Similar phenomena can also be expected when the device is driven by a microwave [48] instead of the electron-phonon coupling.

Acknowledgments.—This work was supported by NSFC (Grant Nos. 11325417, 11674139, and 11574007) and NBRP of China (2015CB921102).

* fangtiefeng@lzu.edu.cn
† luohg@lzu.edu.cn

[1] M. Schleier-Smith, Phys. Rev. Lett. 117, 100001 (2016), and the references wherein.
[2] R. Fazio and R. Raimondi, Phys. Rev. Lett. **80**, 2913 (1998).
[3] Q.-f. Sun, H. Guo, and T.-h. Lin, Phys. Rev. Lett. **87**,

176601 (2001).
[4] A. A. Clerk, V. Ambegaokar, and S. Hershfield, Phys. Rev. B **61**, 3555 (2000); J. C. Cuevas, A. Levy Yeyati, and A. Martín-Rodero, Phys. Rev. B **63**, 094515 (2001); T. Domański, A. Donabidowicz, and K. I. Wysokiński, Phys. Rev. B **76**, 104514 (2007); T. Domański and A. Donabidowicz, Phys. Rev. B **78**, 073105 (2008).
[5] Y. Tanaka, N. Kawakami, and A. Oguri, J. Phys. Soc. Jpn. **76**, 074701 (2007).
[6] Y. Yamada, Y. Tanaka, and N. Kawakami, Phys. Rev. B **84**, 075484 (2011).
[7] J. Barański and T. Domański, J. Phys.: Condens. Matter **25**, 435305 (2013).
[8] A. Koga, Phys. Rev. B **87**, 115409 (2013).
[9] R. Žitko, J. S. Lim, R. López, and R. Aguado, Phys. Rev. B **91**, 045441 (2015).
[10] L. Li, Z. Cao, H.-G. Luo, F.-C. Zhang, and W.-Q. Chen, Phys. Rev. B **92**, 195155 (2015).
[11] T Domański, I. Weymann, M. Barańska, and G. Górski, Sci. Rep. **6**, 23336 (2016).
[12] M. R. Graber, T. Nussbaumer, W. Belzig, and C. Shonenberger, Nanotechnology **15**, S479 (2004).
[13] R. S. Deacon, Y. Tanaka, A. Oiwa, R. Sakano, K. Yoshida, K. Shibata, K. Hirakawa, and S. Tarucha, Phys. Rev. Lett. **104**, 076805 (2010).
[14] R. S. Deacon, Y. Tanaka, A. Oiwa, R. Sakano, K. Yoshida, K. Shibata, K. Hirakawa, and S. Tarucha, Phys. Rev. B **81**, 121308(R) (2010).
[15] A. F. Andreev, Zh. Eksp. Teor. Fiz. **46**, 1823 (1964) [Sov. Phys. JETP **19**, 1228 (1964)].
[16] A. C. Hewson, *The Kondo Problem to Heavy Fermions* (Cambridge University Press, Cambridge, 1993).
[17] M. A. Reed, C. Zhou, C. J. Muller, T. P. Burgin, and J. M. Tour, Science **278**, 252 (1997).
[18] H. Park, M. Lim, E. Anderson, A. Allvisatos, and P. M. Euen, Nature (London) **407**, 57 (2000).
[19] M. Di Ventra, S.-G. Kim, S. T. Pantelides, and N. D. Lang, Phys. Rev. Lett. **86**, 288 (2001).
[20] B. J. LeRoy, S. G. Lemay, J. Kong, and C. Dekker, Nature (London) **432**, 371 (2004).
[21] S. Sapmaz, P. Jarillo-Herrero, Ya. M. Blanter, C. Dekker, and H. S. J. van der Zant, Phys. Rev. Lett. **96**, 026801 (2006).
[22] A. K. Hüttel, B. Witkamp, M. Leijnse, M. R. Wegewijs, and H. S. J. van der Zant, Phys. Rev. Lett. **102**, 225501 (2009).
[23] R. Leturcq, C. Stampfer, K. Inderbitzin, L. Durrer, C. Hierold, E. Mariant, M. G. Schultz, F. von Oppen, and K. Ensslin, Nat. Phys. **5**, 327 (2009).
[24] L. Bai, Z.-Z. Zhang, and L. Jiang, Phys. Lett. A **375**, 661 (2011).
[25] J. Barański and T. Domański, Chin. Phys. B **24**, 017304 (2015).
[26] K. Bocian and W. Rudzinski, Eur. Phys. J. B **88**, 50 (2015).
[27] Q. Wang, H. Xie, H. Jiao, and Y.-H. Nie, Europhys. Lett. **101**, 47008 (2013).
[28] P. Stadler, W. Belzig, and G. Rastelli, arXiv:1511.04858 (unpublished).
[29] P. Zhang and Y.-X. Li, J. Phys.: Condens. Matter **21**, 095602 (2009).
[30] K. F. Albrecht, H. Soller, L. Muhlbacher, and A. Komnik, Phys. E **54**, 15 (2013).
[31] S.-N. Zhang, W. Pei, T.-F. Fang, and Q.-f. Sun, Phys. Rev. B **86**, 104513 (2012).
[32] J. Barański and T. Domański, J. Phys.: Condens. Matter **27**, 305302 (2015).
[33] J. Gramich, A. Baumgartner, and C. Schönenberger, Phys. Rev. Lett. **115**, 216801 (2015).
[34] J. König, H. Schoeller, and G. Schön, Phys. Rev. Lett. **76**, 1715 (1996).
[35] Z.-Z. Chen, H. Lu, R. Lü, and B.-f. Zhu, J. Phys.: Condens. Matter **18**, 5435 (2006).
[36] I. Fernández-Torrente, K. J. Franke, and J. I. Pascual, Phys. Rev. Lett. **101**, 217203 (2008).
[37] Z.-Z. Chen, R. Lü, and B.-f. Zhu, Phys. Rev. B **71**, 165324 (2005).
[38] M. Galperin, A. Nitzan, and M. A. Ratner, Phys. Rev. B **73**, 045314 (2006); Phys. Rev. B **76**, 035301 (2007).
[39] T.-F. Fang, Q.-f. Sun, and H.-G. Luo, Phys. Rev. B **84**, 155417 (2011).
[40] H. Haug and A.-P. Jauho, *Quantum Kinetics in Transport and Optics of Semiconductors*, 2nd ed. (Springer, Berlin, 2008).
[41] Q.-f. Sun, J. Wang, and T.-h. Lin, Phys. Rev. B **62**, 648 (2000).
[42] I. G. Lang and Y. A. Firsov, Sov. Phys. JETP **16**, 1301 (1963).
[43] David M.-T. Kuo and Y. C. Chang, Phys. Rev. B **66**, 085311 (2002); U. Lundin and R. H. McKenzie, Phys. Rev. B **66**, 075303 (2002); A. S. Alexandrov and A. M. Bratkovsky, Phys. Rev. B **67**, 235312 (2003); Y.-S. Liu, H. Chen, X.-H. Fan, and X.-F. Yang, Phys. Rev. B **73**, 115310 (2006); Q.-f. Sun and X. C. Xie, Phys. Rev. B **75**, 155306 (2007); J. Liu, J. Song, Q.-f. Sun, and X. C. Xie, Phys. Rev. B **79**, 161309(R) (2009); L.-L. Zhou, S.-S. Li, J.-N. Wei, and S.-Q. Wang, Phys. Rev. B **83**, 195303 (2011).
[44] G. D. Mahan, *Many-Particle Physics*, 3rd ed. (Plenum, New York, 2000).
[45] T.-K. Ng, Phys. Rev. Lett. **76**, 487 (1996).
[46] In nonequilibrium, one of the proposed schemes to determine the interacting lesser (greater) self-energy $\tilde{\mathbf{\Sigma}}^{<(>)}$ is the Ng's ansatz [45] which has been widely employed in N-QD-N systems, as well as in N-QD-S cases [2, 3]. However, the feasibility of this ansatz on the latter system is not such self-evident. Instead, we approximate $\tilde{\mathbf{\Sigma}}^{<(>)}$ by their noninteracting counterparts $\tilde{\mathbf{\Sigma}}_0^{<(>)}$, which is considered to be reliable to capture our predictions at qualitative level.
[47] D. Chevallier, J. Rech, T. Jonckheere, and T. Martin, Phys. Rev. B **83**, 125421 (2011).
[48] S. Y. Cho, K. Kang, and C.-M. Ryu, Phys. Rev. B **60**, 16874 (1999).